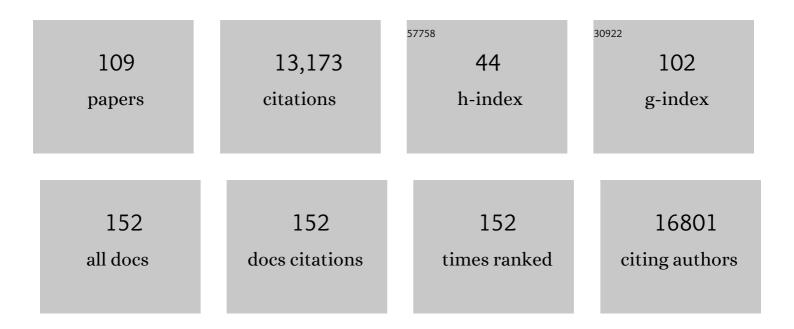
List of Publications by Year in descending order

Source: https://exaly.com/author-pdf/7451893/publications.pdf Version: 2024-02-01



JOHN L PURINETEIN

#	Article	IF	CITATIONS
1	cryoSPARC: algorithms for rapid unsupervised cryo-EM structure determination. Nature Methods, 2017, 14, 290-296.	19.0	5,371
2	Porphysome nanovesicles generated by porphyrin bilayers for use as multimodal biophotonic contrast agents. Nature Materials, 2011, 10, 324-332.	27.5	1,219
3	Structure and conformational states of the bovine mitochondrial ATP synthase by cryo-EM. ELife, 2015, 4, e10180.	6.0	264
4	Electron cryomicroscopy observation of rotational states in a eukaryotic V-ATPase. Nature, 2015, 521, 241-245.	27.8	261
5	Alignment of cryo-EM movies of individual particles by optimization of image translations. Journal of Structural Biology, 2015, 192, 188-195.	2.8	252
6	The structural basis of modified nucleosome recognition by 53BP1. Nature, 2016, 536, 100-103.	27.8	201
7	Structure of the mitochondrial ATP synthase by electron cryomicroscopy. EMBO Journal, 2003, 22, 6182-6192.	7.8	199
8	Structure of the alternative complex III in a supercomplex with cytochrome oxidase. Nature, 2018, 557, 123-126.	27.8	198
9	Atomic model for the dimeric F _O region of mitochondrial ATP synthase. Science, 2017, 358, 936-940.	12.6	194
10	Structure of V-ATPase from the mammalian brain. Science, 2020, 367, 1240-1246.	12.6	153
11	The human coronavirus HCoV-229E S-protein structure and receptor binding. ELife, 2019, 8, .	6.0	153
12	Eukaryotic V-ATPase: Novel structural findings and functional insights. Biochimica Et Biophysica Acta - Bioenergetics, 2014, 1837, 857-879.	1.0	150
13	Atomic model for the membrane-embedded VO motor of a eukaryotic V-ATPase. Nature, 2016, 539, 118-122.	27.8	141
14	Tilt-Pair Analysis of Images from a Range of Different Specimens in Single-Particle Electron Cryomicroscopy. Journal of Molecular Biology, 2011, 413, 1028-1046.	4.2	138
15	Structure of a bacterial ATP synthase. ELife, 2019, 8, .	6.0	133
16	Inhibition of mitochondrial translation overcomes venetoclax resistance in AML through activation of the integrated stress response. Science Translational Medicine, 2019, 11, .	12.4	129
17	Adaptor Protein Self-Assembly Drives the Control of a Cullin-RING Ubiquitin Ligase. Structure, 2012, 20, 1141-1153.	3.3	127
18	Structure of a AAA+ unfoldase in the process of unfolding substrate. ELife, 2017, 6, .	6.0	119

#	Article	IF	CITATIONS
19	The Polydispersity of αB-Crystallin Is Rationalized by an Interconverting Polyhedral Architecture. Structure, 2011, 19, 1855-1863.	3.3	116
20	Structure and Roles of V-type ATPases. Trends in Biochemical Sciences, 2020, 45, 295-307.	7.5	115
21	Molecular basis of human CD22 function and therapeutic targeting. Nature Communications, 2017, 8, 764.	12.8	114
22	Assembly and structural analysis of a covalently closed nano-scale DNA cage. Nucleic Acids Research, 2008, 36, 1113-1119.	14.5	112
23	Arrangement of subunits in intact mammalian mitochondrial ATP synthase determined by cryo-EM. Proceedings of the National Academy of Sciences of the United States of America, 2012, 109, 11675-11680.	7.1	112
24	An Autoinhibited Structure of α-Catenin and Its Implications for Vinculin Recruitment to Adherens Junctions. Journal of Biological Chemistry, 2013, 288, 15913-15925.	3.4	110
25	Structure of mycobacterial ATP synthase bound to the tuberculosis drug bedaquiline. Nature, 2021, 589, 143-147.	27.8	110
26	Subnanometre-resolution structure of the intact Thermus thermophilus H+-driven ATP synthase. Nature, 2012, 481, 214-218.	27.8	109
27	Radiation Damage in Electron Cryomicroscopy. Methods in Enzymology, 2010, 481, 371-388.	1.0	107
28	Bacterial polysaccharide co-polymerases share a common framework for control of polymer length. Nature Structural and Molecular Biology, 2008, 15, 130-138.	8.2	103
29	Structure of a functional obligate complex III2IV2 respiratory supercomplex from Mycobacterium smegmatis. Nature Structural and Molecular Biology, 2018, 25, 1128-1136.	8.2	95
30	A processive rotary mechanism couples substrate unfolding and proteolysis in the ClpXP degradation machinery. ELife, 2020, 9, .	6.0	94
31	Fabrication of carbon films with â^1⁄4500nm holes for cryo-EM with a direct detector device. Journal of Structural Biology, 2014, 185, 42-47.	2.8	92
32	Structure of the vacuolar-type ATPase from Saccharomyces cerevisiae at 11-Ã resolution. Nature Structural and Molecular Biology, 2012, 19, 1356-1362.	8.2	90
33	TROSY-Based NMR Evidence for a Novel Class of 20S Proteasome Inhibitors. Biochemistry, 2008, 47, 6727-6734.	2.5	74
34	The resolution dependence of optimal exposures in liquid nitrogen temperature electron cryomicroscopy of catalase crystals. Journal of Structural Biology, 2010, 169, 431-437.	2.8	73
35	Structural comparison of the vacuolar and Golgi V-ATPases from <i>Saccharomyces cerevisiae</i> . Proceedings of the National Academy of Sciences of the United States of America, 2019, 116, 7272-7277.	7.1	73
36	Electron-event representation data enable efficient cryoEM file storage with full preservation of spatial and temporal resolution. IUCrJ, 2020, 7, 860-869.	2.2	71

#	Article	IF	CITATIONS
37	Structure of intact <i>Thermus thermophilus</i> V-ATPase by cryo-EM reveals organization of the membrane-bound V _O motor. Proceedings of the National Academy of Sciences of the United States of America, 2010, 107, 1367-1372.	7.1	69
38	Cryo-EM Structure of the Yeast ATP Synthase. Journal of Molecular Biology, 2008, 382, 1256-1264.	4.2	62
39	Phospholipid Association Is Essential for Dynamin-related Protein Mgm1 to Function in Mitochondrial Membrane Fusion. Journal of Biological Chemistry, 2009, 284, 28682-28686.	3.4	62
40	The Crystal Structure of Bacteriophage HK97 gp6: Defining a Large Family of Head–Tail Connector Proteins. Journal of Molecular Biology, 2010, 395, 754-768.	4.2	62
41	Shake-it-off: a simple ultrasonic cryo-EM specimen-preparation device. Acta Crystallographica Section D: Structural Biology, 2019, 75, 1063-1070.	2.3	58
42	Reversible inhibition of the ClpP protease via an N-terminal conformational switch. Proceedings of the United States of America, 2018, 115, E6447-E6456.	7.1	56
43	Unfolding the mechanism of the AAA+ unfoldase VAT by a combined cryo-EM, solution NMR study. Proceedings of the National Academy of Sciences of the United States of America, 2016, 113, E4190-9.	7.1	55
44	ATP Synthase from Saccharomyces cerevisiae: Location of the OSCP Subunit in the Peripheral Stalk Region. Journal of Molecular Biology, 2002, 321, 613-619.	4.2	54
45	Molecular basis for the binding and modulation of V-ATPase by a bacterial effector protein. PLoS Pathogens, 2017, 13, e1006394.	4.7	53
46	Automated particle picking for low-contrast macromolecules in cryo-electron microscopy. Journal of Structural Biology, 2014, 186, 1-7.	2.8	52
47	Validating maps from single particle electron cryomicroscopy. Current Opinion in Structural Biology, 2015, 34, 135-144.	5.7	50
48	Multivalency transforms SARS-CoV-2 antibodies into ultrapotent neutralizers. Nature Communications, 2021, 12, 3661.	12.8	48
49	Structure of the Pseudomonas aeruginosa Type IVa Pilus Secretin at 7.4ÂÃ Structure, 2016, 24, 1778-1787.	3.3	47
50	Models for the a subunits of the <i>Thermus thermophilus</i> V/A-ATPase and <i>Saccharomyces cerevisiae</i> V-ATPase enzymes by cryo-EM and evolutionary covariance. Proceedings of the National Academy of Sciences of the United States of America, 2016, 113, 3245-3250.	7.1	47
51	Structural Insights into KCTD Protein Assembly and Cullin3 Recognition. Journal of Molecular Biology, 2016, 428, 92-107.	4.2	47
52	An allosteric switch regulates <i>Mycobacterium tuberculosis</i> ClpP1P2 protease function as established by cryo-EM and methyl-TROSY NMR. Proceedings of the National Academy of Sciences of the United States of America, 2020, 117, 5895-5906.	7.1	47
53	Revised subunit order of mammalian septin complexes explains their in vitro polymerization properties. Molecular Biology of the Cell, 2021, 32, 289-300.	2.1	47
54	Cryo-EM of ATP synthases. Current Opinion in Structural Biology, 2018, 52, 71-79.	5.7	46

JOHN L RUBINSTEIN

#	Article	IF	CITATIONS
55	The RNF168 paralog RNF169 defines a new class of ubiquitylated histone reader involved in the response to DNA damage. ELife, 2017, 6, .	6.0	44
56	Activity-Independent Discovery of Secondary Metabolites Using Chemical Elicitation and Cheminformatic Inference. ACS Chemical Biology, 2015, 10, 2616-2623.	3.4	43
57	The N Termini of a-Subunit Isoforms Are Involved in Signaling between Vacuolar H+-ATPase (V-ATPase) and Cytohesin-2*. Journal of Biological Chemistry, 2013, 288, 5896-5913.	3.4	42
58	YphC and YsxC GTPases assist the maturation of the central protuberance, GTPase associated region and functional core of the 50S ribosomal subunit. Nucleic Acids Research, 2016, 44, 8442-8455.	14.5	42
59	Beyond blob-ology. Science, 2014, 345, 617-619.	12.6	40
60	Structural analysis of membrane protein complexes by single particle electron microscopy. Methods, 2007, 41, 409-416.	3.8	39
61	ATP Synthase from Saccharomyces cerevisiae: Location of Subunit h in the Peripheral Stalk Region. Journal of Molecular Biology, 2005, 345, 513-520.	4.2	38
62	Phages have adapted the same protein fold to fulfill multiple functions in virion assembly. Proceedings of the National Academy of Sciences of the United States of America, 2010, 107, 14384-14389.	7.1	37
63	Cryo-EM structure and kinetics reveal electron transfer by 2D diffusion of cytochrome <i>c</i> in the yeast III-IV respiratory supercomplex. Proceedings of the National Academy of Sciences of the United States of America, 2021, 118, .	7.1	33
64	Electron cryomicroscopy of membrane proteins: Specimen preparation for two-dimensional crystals and single particles. Micron, 2011, 42, 107-116.	2.2	31
65	Cooperative subunit dynamics modulate p97 function. Proceedings of the National Academy of Sciences of the United States of America, 2019, 116, 158-167.	7.1	31
66	Through-grid wicking enables high-speed cryoEM specimen preparation. Acta Crystallographica Section D: Structural Biology, 2020, 76, 1092-1103.	2.3	31
67	Recognition of Semaphorin Proteins by P.Âsordellii Lethal Toxin Reveals Principles of Receptor Specificity in Clostridial Toxins. Cell, 2020, 182, 345-356.e16.	28.9	29
68	Triggered Instability of Liposomes Bound to Hydrophobically Modified Coreâ^'Shell PNIPAM Hydrogel Beads. Langmuir, 2010, 26, 1081-1089.	3.5	28
69	Description and comparison of algorithms for correcting anisotropic magnification in cryo-EM images. Journal of Structural Biology, 2015, 192, 209-215.	2.8	27
70	TMaCS: A hybrid template matching and classification system for partially-automated particle selection. Journal of Structural Biology, 2013, 181, 234-242.	2.8	25
71	Processing of Cryo-EM Movie Data. Methods in Enzymology, 2016, 579, 103-124.	1.0	25
72	Structure of Ycf1p reveals the transmembrane domain TMD0 and the regulatory region of ABCC transporters. Proceedings of the National Academy of Sciences of the United States of America, 2021, 118	7.1	24

#	Article	IF	CITATIONS
73	A Bayesian method for 3D macromolecular structure inference using class average images from single particle electron microscopy. Bioinformatics, 2010, 26, 2406-2415.	4.1	20
74	Apoptolidin family glycomacrolides target leukemia through inhibition of ATP synthase. Nature Chemical Biology, 2022, 18, 360-367.	8.0	20
75	Structure of ATP synthase under strain during catalysis. Nature Communications, 2022, 13, 2232.	12.8	20
76	Cryo-EM studies of the structure and dynamics of vacuolar-type ATPases. Science Advances, 2016, 2, e1600725.	10.3	19
77	An intrinsically disordered motif regulates the interaction between the p47 adaptor and the p97 AAA+ ATPase. Proceedings of the National Academy of Sciences of the United States of America, 2020, 117, 26226-26236.	7.1	19
78	Structure of mycobacterial CIII2CIV2 respiratory supercomplex bound to the tuberculosis drug candidate telacebec (Q203). ELife, 2021, 10, .	6.0	19
79	Vma9p Need Not Be Associated with the Yeast V-ATPase for Fully-Coupled Proton Pumping Activity in Vitro. Biochemistry, 2015, 54, 853-858.	2.5	16
80	Multiple conformations facilitate PilT function in the type IV pilus. Nature Communications, 2019, 10, 5198.	12.8	16
81	Protocol for rapid unsupervised cryo-EM structure determination using cryoSPARC software. Protocol Exchange, 0, , .	0.3	16
82	Detection and quantification of the vacuolar H+ATPase using the <i>Legionella</i> effector protein SidK. Journal of Cell Biology, 2022, 221, .	5.2	16
83	Coordinated conformational changes in the V1 complex during V-ATPase reversible dissociation. Nature Structural and Molecular Biology, 2022, 29, 430-439.	8.2	16
84	Rieske head domain dynamics and indazole-derivative inhibition of Candida albicans complex III. Structure, 2022, 30, 129-138.e4.	3.3	15
85	Structural ordering of the Plasmodium berghei circumsporozoite protein repeats by inhibitory antibody 3D11. ELife, 2020, 9, .	6.0	15
86	Angle determination for side views in single particle electron microscopy. Journal of Structural Biology, 2008, 162, 260-270.	2.8	13
87	CryoEM Reveals the Complexity and Diversity of ATP Synthases. Frontiers in Microbiology, 0, 13, .	3.5	13
88	A pH-Dependent Conformational Switch Controls <i>N. meningitidis</i> ClpP Protease Function. Journal of the American Chemical Society, 2020, 142, 20519-20523.	13.7	12
89	Toosendanin, a novel potent vacuolar-type H ⁺ -translocating ATPase inhibitor, sensitizes cancer cells to chemotherapy by blocking protective autophagy. International Journal of Biological Sciences, 2022, 18, 2684-2702.	6.4	12
90	Use of phage display and high-density screening for the isolation of an antibody against the 51-kDa subunit of complex I. Analytical Biochemistry, 2003, 314, 294-300.	2.4	11

#	Article	IF	CITATIONS
91	Location of Subunit d in the Peripheral Stalk of the ATP Synthase from <i>Saccharomyces cerevisiae</i> . Biochemistry, 2008, 47, 11804-11810.	2.5	11
92	Single Particle Electron Microscopy. Methods in Molecular Biology, 2013, 955, 401-426.	0.9	11
93	CryoEM map of Pseudomonas aeruginosa PilQ enables structural characterization of TsaP. Structure, 2021, 29, 457-466.e4.	3.3	9
94	Cryo-EM Captures the Dynamics of Ion Channel Opening. Cell, 2017, 168, 341-343.	28.9	8
95	Band 3 function and dysfunction in a structural context. Current Opinion in Hematology, 2018, 25, 163-170.	2.5	8
96	The respiratory supercomplex from C.Âglutamicum. Structure, 2022, 30, 338-349.e3.	3.3	7
97	Edged watershed segmentation: A semi-interactive algorithm for segmentation of low-resolution maps from electron cryomicroscopy. Journal of Structural Biology, 2011, 176, 127-132.	2.8	6
98	The study of vacuolar-type ATPases by single particle electron microscopy. Biochemistry and Cell Biology, 2014, 92, 460-466.	2.0	5
99	Structural basis of Plasmodium vivax inhibition by antibodies binding to the circumsporozoite protein repeats. ELife, 2022, 11, .	6.0	5
100	SINGLE PARTICLE ELECTRON MICROSCOPY OF THE MITOCHONDRIAL ATP SYNTHASE. Biophysical Reviews and Letters, 2010, 05, 59-71.	0.8	4
101	Probing Cooperativity of Nâ€Terminal Domain Orientations in the p97 Molecular Machine: Synergy Between NMR Spectroscopy and Cryoâ€EM. Angewandte Chemie - International Edition, 2020, 59, 22423-22426.	13.8	4
102	Cryo-EM of the Yeast V _O Complex Reveals Distinct Binding Sites for Macrolide V-ATPase Inhibitors. ACS Chemical Biology, 2022, 17, 619-628.	3.4	4
103	Flexibility leads to function. Nature Chemistry, 2014, 6, 170-171.	13.6	1
104	Probing Cooperativity of Nâ€Terminal Domain Orientations in the p97 Molecular Machine: Synergy Between NMR Spectroscopy and Cryoâ€EM. Angewandte Chemie, 2020, 132, 22609-22612.	2.0	1
105	Structural Characterization of Endogenous Tuberous Sclerosis Protein Complex Revealed Potential Polymeric Assembly. Biochemistry, 2021, 60, 1808-1821.	2.5	1
106	Through-grid wicking enables high-speed cryoEM specimen preparation. Microscopy and Microanalysis, 2021, 27, 526-528.	0.4	1
107	Algorithmic Advances in Single Particle Cryo-EM Data Processing. Microscopy and Microanalysis, 2018, 24, 868-869.	0.4	0
108	Structure of the Alternative Complex III from <i>Flavobacterium johnsoniae</i> in a Supercomplex with Cytochrome <i>c</i> Oxidase. FASEB Journal, 2020, 34, 1-1.	0.5	0

#	Article	IF	CITATIONS
109	Membrane Protein Structure Determination by Electron Cryo-Microscopy. , 0, , 29-54.		0